Journal of Experimental Botany, Vol. 65, No. 13, pp. 3683–3693, 2014
doi:10.1093/jxb/eru205 Advance Access publication 23 May, 2014
This paper is available online free of all access charges (see http://jxb.oxfordjournals.org/open_access.html for further details)

Journal of Experimental Botany
www.jxb.oxfordjournals.org

RESEARCH PAPER

Increasing water use efficiency along the C_3 to C_4 evolutionary pathway: a stomatal optimization perspective

Danielle A. Way[1,2,*], Gabriel G. Katul[2,3], Stefano Manzoni[4,5,6] and Giulia Vico[4]

[1] Department of Biology, Western University, London, ON, Canada
[2] Nicholas School of the Environment, Duke University, Durham, NC, USA
[3] Department of Civil and Environmental Engineering, Duke University, Durham, NC, USA
[4] Department of Crop Production Ecology, Swedish University of Agricultural Sciences, Uppsala, Sweden
[5] Department of Ecology, Swedish University of Agricultural Sciences, Uppsala, Sweden
[6] Department of Physical Geography and Quaternary Geology, Stockholm University, Stockholm, Sweden.

* To whom correspondence should be addressed. E-mail: dway4@uwo.ca

Received 30 December 2013; Revised 8 April 2014; Accepted 15 April 2014

Abstract

C_4 photosynthesis evolved independently numerous times, probably in response to declining atmospheric CO_2 concentrations, but also to high temperatures and aridity, which enhance water losses through transpiration. Here, the environmental factors controlling stomatal behaviour of leaf-level carbon and water exchange were examined across the evolutionary continuum from C_3 to C_4 photosynthesis at current (400 µmol mol^{-1}) and low (280 µmol mol^{-1}) atmospheric CO_2 conditions. To this aim, a stomatal optimization model was further developed to describe the evolutionary continuum from C_3 to C_4 species within a unified framework. Data on C_3, three categories of C_3–C_4 intermediates, and C_4 *Flaveria* species were used to parameterize the stomatal model, including parameters for the marginal water use efficiency and the efficiency of the CO_2-concentrating mechanism (or C_4 pump); these two parameters are interpreted as traits reflecting the stomatal and photosynthetic adjustments during the C_3 to C_4 transformation. Neither the marginal water use efficiency nor the C_4 pump strength changed significantly from C_3 to early C_3–C_4 intermediate stages, but both traits significantly increased between early C_3–C_4 intermediates and the C_4-like intermediates with an operational C_4 cycle. At low CO_2, net photosynthetic rates showed continuous increases from a C_3 state, across the intermediates and towards C_4 photosynthesis, but only C_4-like intermediates and C_4 species (with an operational C_4 cycle) had higher water use efficiencies than C_3 *Flaveria*. The results demonstrate that both the marginal water use efficiency and the C_4 pump strength increase in C_4 *Flaveria* to improve their photosynthesis and water use efficiency compared with C_3 species. These findings emphasize that the advantage of the early intermediate stages is predominantly carbon based, not water related.

Key words: C_3–C_4 intermediates, C_3 photosynthesis, leaf gas exchange, photosynthetic model, stomatal conductance, water use efficiency.

Introduction

While only 3% of the world's terrestrial plant species use the C_4 photosynthetic pathway, C_4 species are responsible for some 20% of global gross primary productivity (Sage *et al.*, 2012). The high productivity of C_4 plants is due to their efficient photosynthetic physiology, which includes an additional yet spatially separated metabolic cycle, mediated by phospho*enol*pyruvate carboxylase (PEPCase), to the conventional C_3 Calvin–Benson cycle. This additional cycle results

in high CO_2 concentrations around Rubisco, thus suppressing the enzyme's oxygenase function and nearly eliminating photorespiration and the associated carbon and energetic costs.

C_4 photosynthesis has evolved independently at least 66 times in lineages throughout the plant kingdom and, in some of these lines, there are intermediate species that are neither C_3 nor fully C_4 (Sage *et al.*, 2012). Phylogenetic analyses in some evolutionary groups where the full range of C_3, C_3–C_4 intermediates, and C_4 species are found (such as the genus *Flaveria*) have confirmed that C_3 photosynthesis is the basal state and C_4 photosynthesis is more derived; these analyses also place photosynthetic intermediate species as evolutionary intermediates to these two photosynthetic types (McKown *et al.*, 2005). The C_3–C_4 intermediates can be classified into three categories based on the degree to which they express C_4 traits: Type I intermediates show refixation of photorespiratory CO_2 by Rubisco in enlarged bundle sheath cells; Type II species have increased PEPCase activity and some C_4 cycle function; and C_4-like species have an operational C_4 cycle, but have some residual Rubisco activity in their mesophyll cells (Edwards and Ku, 1987).

Despite extensive research, the role of environmental factors in driving the evolution of C_4 photosynthetic traits continues to draw significant attention (e.g. Osborne and Sack, 2012; Griffiths *et al.*, 2013). Much work has focused on the importance of a drop in atmospheric CO_2 concentrations (c_a) from near 1000 ppm to ~400 ppm ~30 million years ago (mya), where the predominant benefit from a CO_2-concentrating mechanism would have been enhanced net CO_2 fixation rates through suppression of photorespiration (Ehleringer *et al.*, 1997; Sage, 2004; Christin *et al.*, 2011; Gowik *et al.*, 2011; Sage *et al.*, 2012). While low c_a increases photorespiration, the effect is even greater when combined with high temperatures: very low c_a conditions, such as those of the last glacial period (~180 μmol mol^{-1}) (Lüthi *et al.*, 2008), may have selected for traits in some C3 species to favour the capture and reassimilation of respired and photorespired CO_2 to offset this stress (Busch *et al.*, 2013), but the detrimental effects of low c_a conditions on C_3 species are further exacerbated at warmer temperatures (Campbell *et al.*, 2005). The warm regions where C_4 species evolved therefore probably stimulated photorespiration considerably, but they also drove a concomitant increase in transpiration demand (Taylor *et al.*, 2012). It has been known for decades that C_4 plants are more water use efficient than C_3 species under the same conditions (e.g. Rawson *et al.*, 1977; Morison and Gifford, 1983); a spate of recent work has highlighted the role of other environmental variables that, along with low c_a, may have contributed to the rise of C_4 photosynthesis, such as dry or saline conditions. These recent studies have emphasized the role of C_4 photosynthesis in improving plant water status and preventing hydraulic failure in these environments (Osborne and Sack, 2012; Griffiths *et al.*, 2013).

Since C_4 species can maintain high photosynthetic rates even when stomatal conductance is low compared with their C_3 counterparts, it follows that C_4 photosynthesis promotes higher water use efficiencies (WUEs) than are found in C_3 species (e.g. Rawson *et al.*, 1977; Morison and Gifford, 1983; Monson, 1989; Huxman and Monson, 2003; Kocacinar *et al.*, 2008; Osborne and Sack, 2012). This pattern is apparent in both forms of WUE: instantaneous WUE (WUE_i, defined as the leaf carbon gain from net photosynthesis, A_{net}, per unit water lost via transpiration, E) and marginal WUE [$\lambda = \frac{\partial A_{net}}{\partial E}$; see Lloyd and Farquhar (1994); Vogan and Sage (2011); Manzoni *et al.* (2011); note that this definition of λ is consistent with that of Hari *et al.* (1986), but the inverse of the same symbol used by Cowan and Farquhar (1977)]. The marginal WUE λ can also be interpreted as the cost of losing water in carbon units. Thus, the higher λ of C_4 species implies that water loss is more costly for the carbon balance with respect to C_3 species, so that C_4 species operate at a relatively low E, but at comparable or higher A_{net}. This finding is consistent with C_4 photosynthesis preventing hydraulic failure by means of a tight stomatal regulation of water loss (Osborne and Sack, 2012). Yet what controls the stomatal behaviour and WUE across the evolutionary continuum of C_3 to C_4 species remains a subject of research (Vogan and Sage, 2011; Way, 2012) and frames the scope of this work.

Recent experiments have shown that instead of a gradual improvement in WUE from C_3 species, across the intermediate range and to a full C_4 pathway, the increase in WUE resembles a threshold effect: Type I and II intermediates have WUEs on a par with C_3 species, while C_4-like species have a high WUE akin to C_4 plants (Kocacinar *et al.*, 2008; Vogan and Sage, 2011). The development of the CO_2-concentrating mechanism, which effectively pumps CO_2 from the substomatal cavity into the chloroplasts where the Calvin–Benson cycle occurs, is thought to be the primary mechanism by which C_4 plants enhance their WUE_i. The present study therefore sought to investigate the connection between the evolutionary continuum of C_3 to C_4 photosynthesis and stomatal behaviour (which is a key factor in controlling WUE), by exploring the following questions.

(i) To what degree can stomatal optimization theories describe the WUE_i patterns in species that have photosynthetic characteristics intermediate between C_3 and C_4 species?
(ii) What are the relationships among the CO_2-concentrating mechanism, λ, and WUE_i in these C_3–C_4 intermediates?

To address these questions, the genus *Flaveria* was used as a case study, since it contains species with C_3 photosynthesis, all three intermediate photosynthetic types, and C_4 photosynthesis (a system previously used by Huxman and Monson, 2003; Sage, 2004; McKown and Dengler, 2007; Kocacinar *et al.*, 2008; Gowik and Westhoff, 2011; Gowik *et al.*, 2011; Vogan and Sage, 2011; and others). Data on *Flaveria* are used to parameterize a stomatal optimization model and examine stomatal behaviour across the evolutionary range of C_3 to C_4 photosynthesis. By using a phylogenetically constrained system, the patterns of changes in the model parameters across the C_3–C_4 photosynthetic continuum can be simultaneously explored while minimizing evolutionary differences between groups that might otherwise confound the analysis.

Theory

In the Farquhar *et al.* (1980) photosynthesis model, A_{net} is determined by the minimum of two limitations: the Rubisco carboxylation rate (A_C) and ribulose-1,5-bisphosphate (RuBP) regeneration rate A_J, and is commonly expressed as

$$A_{net} = \min(A_C, A_J) - R_d, \quad (1)$$

where R_d is the daytime respiration rate (see Table 1 for symbols and definitions). Rubisco limitation occurs under saturating light or at low CO_2 concentrations at the site of Rubisco, while RuBP regeneration tends to limit photosynthesis when c_a is high and light levels are low, resulting in a limited electron transport rate. The Rubisco-limited assimilation rate, A_C, can be expressed as

$$A_C = V_{c,max}\frac{c_c - \Gamma^*}{c_c + K_{cair}}, \quad (2)$$

where $V_{c,max}$ is the maximum Rubisco carboxylation rate, c_c is the CO_2 concentration at the photosynthetic site, Γ^* is the CO_2 compensation point in the absence of mitochondrial respiration, and $K_{cair} = K_c(1 + O/K_o)$, with K_c and K_o being the Michaelis–Menten constants for Rubisco CO_2 fixation and oxygen inhibition, and O is the oxygen concentration in the air (21%). Conversely, the RuBP-limited assimilation rate is constrained by the rate of electron transport, J, and can be expressed as

$$A_J = \frac{J}{4}\frac{c_c - \Gamma^*}{c_c + 2\Gamma^*}, \quad (3)$$

where the electron transport rate is given by $J=\alpha_p\varepsilon_m Q$, and Q is the irradiance, α_p is the leaf absorptivity, and ε_m is the maximum photochemical efficiency (Genty *et al.*, 1989).

To avoid discontinuities in A_{net} due to an abrupt transition from one limitation to another, the minimum function in Equation 1 has often been replaced by a quadratic function, at the cost of introducing an additional curvature parameter. An alternative approach is to approximate Equation 1 by a hyperbolic function (Vico *et al.*, 2013),

$$A_{C,J} = k_1\frac{c_c - \Gamma^*}{c_c + k_2}, \quad (4)$$

where $k_1 = \frac{J}{4}$ and $k_2 = JK_{cair}/(4V_{c,max})$. Such a representation ensures that at low c_c/k_2, $A_{C,J} \approx A_C$ and at large c_c/k_2, $A_{C,J} \approx A_J$. When c_c/k_2 is approximately unity, both Rubisco and RuBP regeneration rates exert comparable limitations on photosynthesis. Hereafter, this regime is referred to as the co-limitation regime. Under CO_2-limited (or light-saturated) conditions in which $k_1=V_{c,max}$ and $k_2=K_{cair}$, the optimal solution is identical to the one obtained by Katul *et al.* (2010) for non-linear photosynthetic kinetics without light limitation. Based on Equation 4, net photosynthesis is obtained as $A_{net}=A_{C,J}-R_d$.

Although there are numerous physiological and anatomical traits that underlie the development of the CO_2-concentrating mechanism in C_4 plants (e.g. McKown and Dengler, 2007; Sage *et al.*, 2012), for modelling purposes, the simplest description of the effect of such a pump is to assume that the CO_2 concentration at the site where photosynthesis occurs is $c_c=\eta c_i$, where η represent the strength of the CO_2-concentrating pump. The value of η encompasses not only the development of C_4 biochemistry across the evolutionary gradient of species, but also biochemical and anatomical features that affect mesophyll conductance. In C_4 species, $\eta>1$ (Manzoni *et al.*, 2011); while it is slightly smaller than unity in C_3 species due to the need to diffuse CO_2 through the mesophyll, the lack of specific data on mesophyll conductance meant this had to be neglected and $\eta=1$ was set for C_3 species.

In the following, the pump strength, η, is estimated from the slope of the $A_{net}(c_i)$ curve. Employing this simple description of the CO_2-concentrating mechanism results in a simpler photosynthesis model than by considering explicitly PEPCase kinetics (Collatz *et al.*, 1992; Laisk and Edwards, 2000; von Caemmerer, 2000, 2013; Vico and Porporato, 2008), thereby allowing data sets collected across different experiments and conditions to be compared. Nevertheless, the parameter η can be linked to the kinetics of PEPCase. The CO_2 concentration in the stomatal cavity (c_i) is assumed to be transported by PEPCase activity and the shuttling of C_4 acids to the bundle sheath (the site of photosynthesis), where the CO_2 concentration reaches c_{bs}. When PEPCase kinetics are assumed to be linear for illustration (but see von Caemmerer, 2000 for more detailed and non-linear models), then

$$V_P = \alpha c_i, \quad (5)$$

where α is the kinetic constant of the process. Setting $V_p=A_{net}$ (from Equation 4) to guarantee continuity in the C fluxes from the stomatal cavity to the site of photosynthesis provides an equation to be solved for η, leading to

$$\eta = \frac{k_1\Gamma^* + k_2(\alpha c_i + R_d)}{c_i(k_1 - \alpha c_i - R_d)}. \quad (6)$$

Equation 6 shows that the pump efficiency η in principle depends on the photosynthetic parameters as well as c_i. However, neglecting R_d and assuming $\Gamma^* \ll c_i$ and $\alpha c_i \ll k_1$, it can be shown that $\eta = \alpha k_2/k_1$, which is a constant at a given temperature and light level. Therefore, when respiration is small and photosynthetic capacity is large, a constant efficiency η captures the main effect of the PEPCase on the photosynthetic rate. Outside these simplifications, the assumption of a constant η can only be regarded as a first-order approximation.

The combination of the hyperbolic function in Equation 4 with the simplified description of the CO_2 pumping mechanism based on η (i.e. $c_c=\eta c_i$) provides a tool to describe CO_2 demand within a common framework valid across the C_3 to C_4 evolutionary continuum. Despite the inherent simplifications, this model is in good agreement with earlier, more complex photosynthesis models for C_3–C_4 intermediates and C_4 species (von Caemmerer, 1989; Collatz *et al.*, 1992) (data not shown; for an example of model comparison for C_3 species, see fig. 1 in Vico *et al.*, 2013), thus lending support to the present approach.

Table 1. *Symbols and their definitions used in the paper and model*

Symbol	Definition	Units
a	Ratio of the molecular diffusivities of CO_2 to water vapour	–
A_C	Rubisco-limited CO_2 assimilation rate	μmol m^{-2} s^{-1}
A_J	RuBP regeneration-limited net CO_2 assimilation rate	μmol m^{-2} s^{-1}
A_{net}	Net CO_2 assimilation rate	μmol m^{-2} s^{-1}
c_a	Atmospheric CO_2 concentration	μmol mol^{-1}
c_{bs}	Bundle sheath CO_2 concentration	μmol mol^{-1}
c_c	Chloroplastic CO_2 concentration	μmol mol^{-1}
CE	Carboxylation efficiency	mol m^{-2} s^{-1}
c_i	Intercellular CO_2 concentration	μmol mol^{-1}
D	Vapour pressure deficit	kPa
E	Transpiration rate	mmol m^{-2} s^{-1}
g_s	Stomatal conductance	mmol m^{-2} s^{-1}
J	Electron transport rate	μmol m^{-2} s^{-1}
k_1	Maximum photosynthetic rate of the hyperbolic model (Equation 4)	μmol m^{-2} s^{-1}
k_2	Half-saturation constant for the hyperbolic model (Equation 4)	–
K_c	Michaelis–Menten constant for Rubisco carboxylation	μmol mol^{-1}
K_{cair}	Half-saturated constant of the Rubisco-limited photosynthesis	μmol mol^{-1}
k_{cat}	Catalytic constant for Rubisco	mol mol^{-1} s^{-1}
K_o	Michaelis–Menten constant for Rubisco oxygenation	mmol mol^{-11}
O	Atmospheric oxygen concentration	mmol mol^{-1}
Q	Irradiance	μmol m^{-2} s^{-1}
q	Temperature coefficient	–
R_d	Day respiration	μmol m^{-2} s^{-1}
T_l	Leaf temperature	°C
$V_{c,max}$	Maximum carboxylation rate of Rubisco	μmol m^{-2} s^{-1}
$V_{c,max25}$	Maximum carboxylation rate of Rubisco at 25 °C	μmol m^{-2} s^{-1}
V_p	PEPCase rate	μmol m^{-2} s^{-1}
WUE	Water use efficiency	mmol mol^{-1}
WUE_i	Instantaneous water use efficiency	mmol mol^{-1}
α	Kinetic constant (Equations 5 and 6)	–
α_p	Leaf absorptivity	–
$\alpha_{1,2}$	Parameter groups (Equations 8–11)	–
$\beta_{1,2,3}$	Parameter groups (Equations 8–11)	–
ε_m	Maximum photochemical efficiency	–
γ	Parameter groups (Equations 8–11)	–
Γ	CO_2 compensation point	μmol mol^{-1}
Γ*	CO_2 compensation point in the absence of mitochondrial respiration	μmol mol^{-1}
η	C4 pump strength	–
λ	Marginal water use efficiency	mmol mol^{-1}

The biochemical demand for CO_2 described by $A_{C,J}$ is met by CO_2 supplied by the atmosphere via Fickian diffusion at a rate given by

$$A_{net} = g_s(c_a - c_i), \quad (7)$$

where g_s is the stomatal conductance and c_a is the atmospheric CO_2 concentration. For a given c_a, set of environmental conditions (such as Q and temperature), and physiological properties determining k_1 and k_2, the atmospheric supply and biochemical demand for $A_{C,J}$ constitute two equations with three unknowns: g_s, c_a, and A_{net}. Hence, one additional equation is needed to close this system of equations mathematically.

This additional equation can take on the form of an optimality rule, whereby stomata are assumed to operate so as to maximize their carbon gain at a given water loss cost (Cowan and Farquhar, 1977; Hari *et al.*, 1986). This hypothesis is equivalent to maximizing a Hamiltonian function $H=A_{net}-\lambda E$, where $E=ag_sD$ is the leaf transpiration rate (assuming a perfectly coupled canopy), and a=1.6 is the ratio of the molecular diffusivities of CO_2 to water vapour. Combining the biochemical demand with atmospheric supply so as to eliminate c_i, and thereby expressing $A_{C,J}$ as a function of g_s, inserting the outcome into the Hamiltonian, and setting $\partial H / \partial g_s=0$, leads to a quadratic equation in g_s (Vico *et al.*, 2013). Solving this equation for g_s results in a solution for optimal g_s as a function of biochemical parameters (η, $V_{c,max}$, K_{cair}, R_d, and Γ*), environmental conditions (c_a and D), and the optimization parameter λ. The explicit functional form for optimal stomatal conductance is determined from the solution to the optimality problem as

$$\frac{\partial H}{\partial g_s}=\frac{\partial (A_{net}-\lambda E)}{\partial g_s}=0 \overset{\text{optimality condition}}{\rightarrow} g_s=\frac{\beta_1+\sqrt{\beta_2}}{\beta_3} \quad (8)$$

where

$$\beta_1=-\gamma\eta(k_2+\alpha_2)\left[k_1(k_2-\eta c_a+2\Gamma^*)+\alpha_1 R_d\right], \quad (9)$$

$$\beta_2=-\gamma\eta k_1(k_2+\Gamma^*)(k_2+\alpha_2)\left[k_2+\eta(c_a-2\gamma)\right]^2\left[k_1(\Gamma^*-\eta c_a)+\alpha_1 R_d\right], \quad (10)$$

$$\beta_3=\gamma\alpha_1^2(k_2+\alpha_2) \quad (11)$$

In Equations 9, 10, and 11, $\alpha_1=k_2+\eta c_a$, $\alpha_2=\eta(c_a-\gamma)$, and $\gamma=\alpha\lambda D$. Therefore, the optimal stomatal conductance depends on λ, which by using the optimization condition $\partial H/\partial g_s=0$ can be shown to be equal to the definition of the marginal WUE, i.e.

$$\lambda=\frac{\partial A_{net}}{\partial E}=\frac{\partial A_{net}}{\partial g_s}\left(\frac{\partial E}{\partial g_s}\right)^{-1}. \quad (12)$$

Equation 12 provides a physical interpretation for λ, but does not give additional information (the optimization condition has already been used in Equation 8). Hence, λ needs to be determined to close the optimization problem mathematically. Although λ changes as a function of time when soil moisture declines during a dry period (Manzoni *et al.*, 2013), under well-watered conditions or stable moisture levels, λ can be considered time-invariant.

Before applying the proposed model, it is important to summarize its key assumptions and simplifications:

(i) Photosynthetic kinetics are described by a hyperbolic function of c_i bridging a CO_2-limited regime (where A_{net} scales linearly with c_i) and a light-limited regime (where A_{net} depends solely on a light level).

(ii) PEPCase kinetics are described by a single efficiency parameter η, which approximates more complex models well (Collatz *et al.*, 1992; von Caemmerer, 2000) when respiration terms are small. Also mesophyll resistance is neglected, due to a lack of data across these species; this assumption implies that the estimated η could be inflated under dry conditions (though these are not the conditions considered when inferring the marginal WUE).

(iii) Stomatal conductance is obtained from an optimization argument assuming that the marginal WUE is constant—a reasonable approximation for experiments under controlled conditions and stable moisture levels (Manzoni *et al.*, 2013). Thus, λ is used as a fitting parameter affecting the stomatal conductance in Equation 8.

Clearly, these assumptions could be relaxed, thereby improving realism. However, relaxing these assumptions reduces the ease of interpretation of the derived equations and the ability to compare across a wide range of data sets due to more required parameters. Once the optimal g_s is determined, $A_{C,J}$, E, and c_i can then be computed. This model allows the quantification of A_{net} and g_s for C_3, C_4, and C_3–C_4 intermediate species within a common framework and as a function of both environmental conditions (air temperature, Q, D, and c_a) and species-specific parameters (η, λ, $V_{c,max}$, K_{cair}, and Γ*)). As such, after showing that the modelled response of A_{net} to changes in g_s is well captured assuming optimal stomatal behaviour, the model is used to investigate how A_{net} and WUE_i are altered by changes in η, λ, and c_a, thus following the steps of the hypothesized evolution of C_3–C_4 intermediates and C_4 species from C_3 plants.

Data availability and model parameterization

To examine the consequences of intermediacy on stomatal behaviour, WUE_i, and λ, *Flaveria* species were used where gas exchange measurements for C_3, C_4, and intermediate species have been previously characterized. The data included C_3 species (*F. cronquistii* and *F. pringlei*), Type I intermediates (*F. angustifolia*, *F. chloraefolia*, *F. pubescens* and *F. sonorensis*), Type II intermediates (*F. floridana* and *F. ramosissima*), C_4-like intermediates (*F. brownii*, *F. palmeri* and *F. vaginata*), and C_4 species (*F. australasica*, *F. bidentis*, *F. kochiana* and *F. trinervia*) (see Supplementary Table S1 available at *JXB* online). The most recent photosynthetic classification of the species (Vogan and Sage, 2011) was employed. Responses of g_s and A_{net} to variation in c_a, and responses of A_{net} to changes in g_s were either taken from the literature or digitized from published graphs (Monson, 1989; Vogan and Sage, 2011). Environmental conditions (Q, D, c_a, and leaf temperature) in model runs were matched to the measurement conditions described for the experimental data. The range in λ necessary to capture measured responses in gas exchange was explored in *Flaveria* species from all photosynthetic types.

To parameterize the above model for *Flaveria*, $V_{c,max}$ values were derived for Rubisco from 15 *Flaveria* species that spanned C_3 to C_4 photosynthetic types using *in vitro* measurements of catalytic constants (or turnover numbers, k_{cat}) (Kubien *et al.*, 2008) and Rubisco site concentrations from the same experiment (D. Kubien, personal communication) (Table 2). The Michaelis–Menten constants K_c and K_o for Rubisco were also taken for each *Flaveria* species from Kubien *et al.* (2008). Rubisco kinetics were adjusted to 30 °C to match conditions in the carboxylation efficiency studies using correction equations and coefficients from Campbell and Norman (1998) (Table 2). K_c and K_o were temperature adjusted by multiplying their values at 25 °C by $\exp[q(T_l-25)]$, where q is the temperature coefficient for that parameter (0.074 for K_c and 0.015 for K_o) and T_l is leaf temperature. $V_{c,max}$ was adjusted as $V_{c,max}=\frac{V_{c,max25}\exp[0.088(T_l-25)]}{1+\exp[0.29(T_l-41)]}$, where $V_{c,max25}$ is the maximum carboxylation rate at 25 °C. The Γ* values for each of the five photosynthetic types were approximated using averaged values of Γ (the CO_2 compensation point) from *Flaveria* species in Ku *et al.* (1991), assuming that day respiration of mitochondria is small ($R_d=0.015V_{c,max}$) and can be ignored (Table 2). Because light conditions varied across experiments, the estimation of $J(\alpha_p\varepsilon_m Q)$ needed

Table 2. *Parameter values (based on mean values from experimental data corrected to 30 °C) used for modelling photosynthesis for each photosynthetic type of* Flaveria

	CE (mol m^{-2} s^{-1})	Γ (μol mol^{-1})	$V_{c,max}$ (μmol m^{-2} s^{-1})	K_c (μmol mol^{-1})	K_o (mmol mol^{-1})	R_d (μmol m^{-2} s^{-1})	λ (mmol mol^{-1})	η (unitless)
References for values	Sudderth *et al.* (2007), citing Dai *et al.* (1996)	Ku *et al.* (1991)	Kubien *et al.* (2008) (and pers. comm.)	Kubien *et al.* (2008)	Kubien *et al.* (2008)	Estimated as 0.015 $V_{c,max}$		
C_3 species	0.11	61.36	53.20	494.9	575.8	0.8	0.826	1.83
Type I	0.079	25.45	73.40	516.6	665.7	1.10	0.739	1.73
Type II	0.13	9.20	66.72	547.1	614.6	1.00	0.754	1.93
C_4-like	0.27	4.93	34.10	690.3	422.3	0.51	3.267	8.83
C_4 species	0.47	3.32	39.52	898.7	1631.8	0.59	3.410	17.60

CE, carboxylation efficiency; Γ, CO_2 compensation point; $V_{c,max}$, *in vitro* maximum carboxylation rate of Rubisco; K_c and K_o (at 30 °C), Rubisco Michaelis–Menten constants for CO_2 and O_2, respectively; R_d, day respiration rates; λ, marginal water use efficiency; η, C_4 pump strength.
Data are taken from literature sources as outlined in the text (see also species-specific data points in Fig. 2 and Supplementary Table S1 at JXB online); λ and η are calculated values.

in determining $a_1 = J$ and $a_2 = Jk_2 / (4V_{c,max})$ requires an estimate of the product $\alpha_p\varepsilon_m$ (not their individual values). The value for α_p was set at 0.8 (based on values for C_3 and C_4 species in von Caemmerer, 2000 and Collatz *et al.*, 1992, respectively), ε_m was 0.1 mol mol^{-1} (similar to Norman and Campbell, 1998; Cheng *et al.*, 2001; Taiz and Zeiger, 2010), and Q was set for the irradiance used in individual papers being modelled. Hence, $\alpha_p\varepsilon_m$=0.08, resulting in α_1=0.08Q when RuBP regeneration limits photosynthesis. This estimate is consistent with conventional values for C_3 species (Campbell and Norman, 1998; see table 14.1) though $\alpha_p\varepsilon_m$ may be more uncertain for C_4 species and C_3–C_4 intermediates. For C_3–C_4 intermediates, Monson (1989) and Monson and Jaeger (1991) report mid-day photosynthetic rates for several species including *F. floridana* between 15 μmol m^{-2} s^{-1} and 45 μmol m^{-2} s^{-1} at light levels ranging from Q=1500 μmol m^{-2} s^{-1} to 2000 μmol m^{-2} s^{-1}. Because $A_J \approx J/4$ (assuming that Γ* is negligible in Equation 3), it follows that the measured A are consistent with the estimate J=0.08Q, which gives an A_{net} of 40 μmol m^{-2} s^{-1}. This evidence supports the assumption that $\alpha_p\varepsilon_m$ is stable across photosynthetic types. A more rigorous parameterization would require direct observations of $\alpha_p\varepsilon_m$ or reliable $V_{c,max}$–J_{max} relationships across the C_3–C_4 continuum.

Carboxylation efficiencies [CEs; i.e, the initial slope of the $A_{net}(c_i)$ curve] measured under saturating light for *Flaveria* species were taken from Krall *et al.* (1991) and Sudderth *et al.* (2007), citing Dai *et al.* (1996). Based on Equation 2, at low c_i the slope of the $A_{net}(c_i)$ is approximately $CE = V_{c,max}\eta / K_{cair}$, so that $\eta = CEK_{cair} / V_{c,max}$. Therefore, knowledge of Γ, K_{cair}, K_c, and K_o allowed an estimate of η for each *Flaveria* species.

Finally, the Vogan and Sage (2011) gas exchange data set was used to infer how λ changes across the evolutionary pathway from C_3 to C_4 species. In that study, a range of g_s and A_{net} values was obtained by altering the nitrogen availability for individuals of all photosynthetic types considered, while water was amply supplied, so λ can be considered time-invariant. As a consequence of different nutrient availability, a range of photosynthetic capacities and respiration rates were obtained. Since there is no way of knowing these biochemical parameters, a simplified but more robust approach to estimate λ was adopted that only requires gas exchange rates and photosynthetic type-averaged Γ and η (assuming λ is substantially unaltered by nutrient availability). For this step, instead of using the definition (Equation 12), which requires knowledge of all the photosynthetic parameters, the stomatal optimization model was simplified by selecting light-saturated conditions, so that $R_d \approx 0$ and the photosynthesis model is approximately linear. Following these simplifications, it can be shown that $A_{net} = g_s\sqrt{aD\lambda(c_a - \Gamma_* / \eta)}$ (Manzoni *et al.*, 2011), which allows estimating λ through a linear least square regression of A_{net} versus g_s constrained through the origin for each photosynthetic type. In previous works on different species, this approach to estimate λ was compared with results obtained without these simplifications. Such comparison showed that the differences between the two approaches was rarely more than 20% across a wide range of environmental and physiological conditions (see fig. 4 in Katul *et al.*, 2010), which is in the range of experimental variability [e.g. a mean standard deviation of 16% in light-saturated A_{net} estimates across individuals in a range of C_3, C_3–C_4 intermediates, and C_4 species (Vogan *et al.*, 2007)].

Gas exchange rates were also simulated under altered atmospheric CO_2 concentrations. In this analysis, all biochemical parameters were maintained constant, but the possibility was considered that the marginal WUE increases linearly with CO_2 concentrations (Manzoni *et al.*, 2011). Simulations with constant λ estimated as described above were thus compared with simulations with $\lambda(c_a)=\lambda_{400}(c_a/400)$. Including CO_2 effects allows the robustness of the results to changes in λ to be tested.

Results and Discussion

Recent work has stimulated new interest in the role that transpiration demands may have played in the evolution of C_4 photosynthesis and traits associated with the C_4 syndrome (Taylor *et al.*, 2011, 2012; Osborne and Sack, 2012; Griffiths

et al., 2013). These studies have emphasized that C_4 photosynthesis not only benefits the carbon economy of a plant, but also has important implications for hydraulic traits, drought tolerance, and water use patterns, benefits that are maintained or enhanced when C_4 plants are exposed to the low c_a conditions where C_4 photosynthesis evolved (Ripley *et al.*, 2013). Here, λ is used as an 'index' of the cost of losing water in terms of carbon, and its variation along the evolutionary gradient from C_3 to C_4 photosynthesis is investigated.

Combining a stomatal optimization approach with measured biochemical parameters, realistic mean $A_{net}(c_i)$ curves for each photosynthetic pathway in *Flaveria* were computed (Fig. 1A; Table 2). The corresponding estimated η values are reported in Fig. 1B. In the optimality model, recall that the parameter η represents an overall pump strength for the carbon-concentrating mechanism, which might naively have been expected to increase gradually from C_3 towards C_4 plants. Instead, the analysis here suggests that η was relatively stable and similar to that for C_3 species (η=1 or slightly above 1 due to unavoidable errors in the estimation) until reaching C_4-like species. The relatively constant η between C_3, Type I, and Type II *Flaveria* species occurred despite there being an increase in the initial slope of the $A_{net}(c_i)$ curve (e.g. the carboxylation efficiency) across these groups. Instead of being attributed to η, the steeper initial slopes in the Type I and Type II intermediates in comparison with the C_3 species were caused by higher $V_{c,max}$ values for Rubisco based on *in vitro* assays of the enzyme kinetic parameters (Table 2; Fig. 2A), consistent with positive selection on Rubisco across the C_3 to C_4 gradient (Kapralov *et al.*, 2011). Thus, there was no increase in η until the C_4-like species were reached; at this point, η values were about half-way between those of the full C_3 and C_4 photosynthetic groups. The greater variation in η estimates in species closer to the C_4 end of the spectrum is therefore probably due to the greater range of pump strengths possible as the carbon-concentrating mechanism is established and to the species-level diversity in $V_{c,max}$ values (Supplementary Table S1 at *JXB* online). While there were sharp changes in *in vitro* Rubisco $V_{c,max}$ between C_3 species and the Type I and Type II intermediates, the change in the K_{cair} of Rubisco across the photosynthetic groups was more gradual until reaching the C_4-like species (Fig. 2B), implying that these enzyme kinetic traits are not necessarily linked. The Γ* dropped sharply as η increased slightly above a value of 1 and then flattened (Fig. 2C).

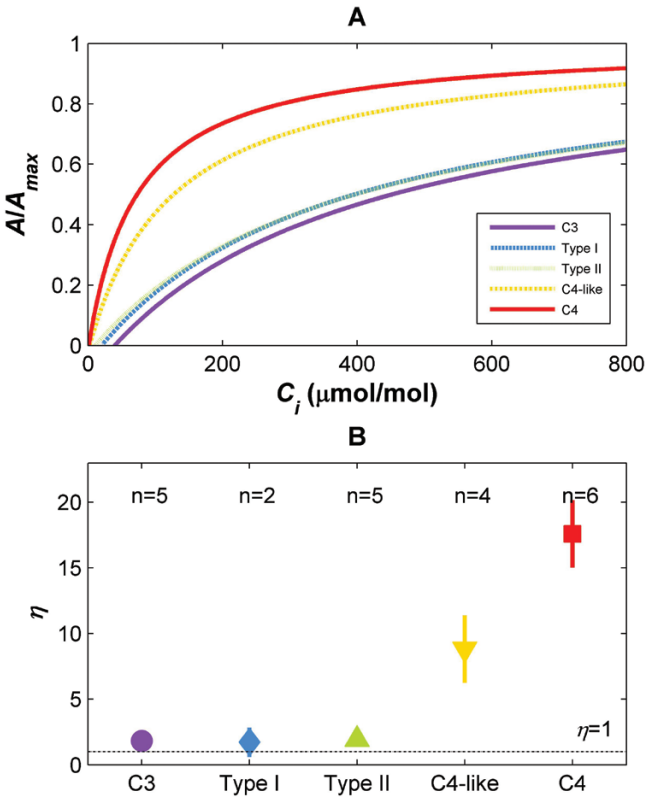

Fig. 1. (A) Responses of net CO_2 assimilation rates (A_{net}) to increases in intercellular CO_2 concentration (c_i), relativized to maximum A_{net} (=A_{max}) for each photosynthetic type, as commonly presented in the literature. (B) Estimated η for each photosynthetic type. Means ±SE, *n* indicated at the top, dotted line indicates η=1. C_3 species, purple circles and solid line; Type I species, blue diamonds and dashed line; Type II species, green triangles and dotted line; C_4-like species, yellow inverted triangles and dashed-dotted line; C_4 species, red squares and solid line.

While it might, *a priori*, seem reasonable to expect a steady increase in WUE_i from C_3 species through the intermediate *Flaveria* species and to full C_4 plants, this was not borne out by the data, in agreement with published findings. Huxman and Monson (2003) showed that the WUE_is of C_3–C_4 intermediates were similar to C_3 WUE_i values, while C_4 WUE_i values were considerably higher. Vogan and Sage (2011) also found no evidence for a gradual transition in the slope between A_{net} and g_s in C_3–C_4 intermediates, but rather a sharp increase between Type II intermediates and C_4-like intermediates. [Note that WUE_i is a proxy for λ if a linear $A_{net}(c_i)$ curve is assumed.] In our re-analysis of the Vogan and Sage (2011) data set, the reported gas exchange data could be readily described with the optimality model for C_3, and Type I and Type II intermediates using the estimated changes in η (as in Fig. 1B), but without significant changes in λ across photosynthetic pathways (Fig. 3). This result implies that there is little change in the relationship between carbon and water from that of a C_3 species in these early intermediate steps. However, in C_4-like intermediates, a strong C_4 pump (i.e. η=8) was accompanied by a quadrupling of λ compared with that used to characterize the data for Type I and II intermediates. Thus, the stomatal optimization approach could be successfully used to capture key changes in the measured relationship between A_{net} and g_s across the C_3–C_4 spectrum using the estimated η values, but only when the marginal WUE of the C_4-like and C_4 species was modelled to be 4-fold greater than that of the C_3 species (Fig. 3). This increase in λ unambiguously indicates a higher carbon cost for losing water in the C_4-like and C_4 species. In the optimization model, the long-term c_i/c_a dictates λ, because $\lambda \infty (1-c_i/c_a)^2$. Therefore, the increase in λ is generated by a decline in c_i (where c_a is assumed to be 400 μmol mol^{-1}). This finding suggests that the increase in C_4 WUE_i values, the increase in λ, and the decline in c_i (as expected by the presence of a C_4 pump) are all interconnected and predicted from the proposed stomatal optimization model.

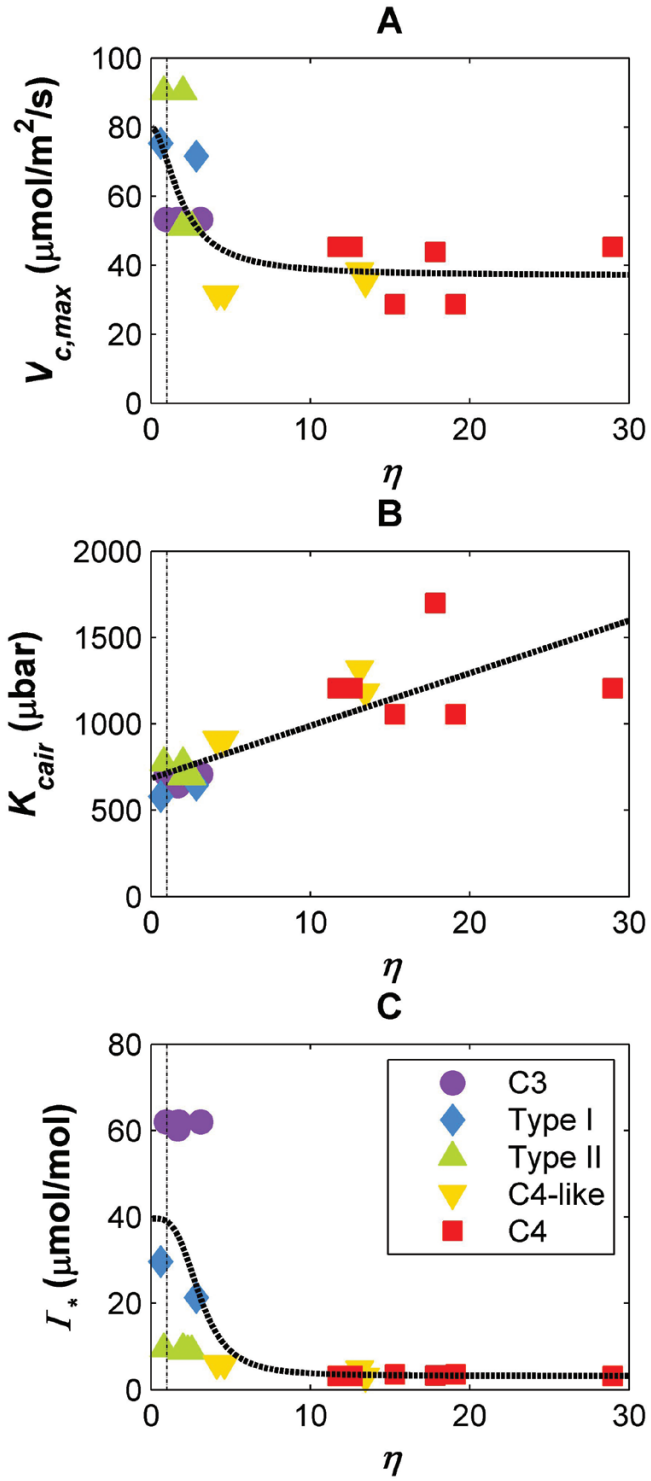

Fig. 2. Relationships between the pump strength of the CO_2-concentrating mechanism (η) and: (A) maximum carboxylation capacity of Rubisco ($V_{c,max}$); (B) $K_{cair} = K_c(1+O/K_o)$; and (C) the CO_2 compensation point in the absence of mitochondrial respiration (Γ*) for C_3, C_4, and C_3–C_4 intermediate species. Solid lines are fit to data; vertical dotted lines indicate η=1. C_3 species, purple circles; Type I species, blue diamonds; Type II species, green triangles; C_4-like species, yellow inverted triangles; C_4 species, red squares.

Since C_4 photosynthesis evolved under low c_a, with the transition in *Flaveria* occurring within the last 3 million years (Sage *et al.*, 2012), the effect of varying η and λ on A_{net} and WUE_i was further investigated under both current (400 μmol mol^{-1}) and low CO_2 concentrations (280 μmol mol^{-1}; Figs 4, 5), allowing $V_{c,max}$, K_{cair}, and Γ* to vary along with η as per the relationships in Figs 1 and 2, but keeping λ constant. In the results from both current and low c_a levels, increases in η initially induce a sharp increase in A_{net}, as more CO_2 is concentrated around Rubisco, with a diminishing response above a certain η (η=10 for 400 μmol mol^{-1} CO_2; Fig. 4A). Moreover, higher values of λ decrease A_{net} in both environments, so that the slight changes in η and λ in Type I and II species compared with C_3 plants generate a similar A_{net} in the three groups (Fig. 4A). Increased c_a (from 280 μmol m^{-2} s^{-1} to 400 μmol mol^{-1}) elevated A_{net} in C_3 species by 80% due to greater substrate availability (Fig. 4B). Compared with a C_3 *Flaveria* at these low c_a, C_3–C_4 intermediates also have higher A_{net} in modern CO_2 concentrations, with a gradual increase in the stimulation of A_{net} with respect to C_3 values (Fig. 4B). In contrast to the A_{net} results, increases in η have little impact on WUE_i when λ is small, namely from C_3 species to Type I or II species (shown for 400 μmol mol^{-1} CO_2 in Fig. 5A). Moreover, while increases in c_a have increased WUE_i of C_3 species by 30%, there is no gradual rise in WUE_i across the gradient of photosynthetic types, as there was with A_{net} (Fig. 5B). Instead, compared with a C_3 *Flaveria* at 280 μmol mol^{-1} CO_2, Type I and Type II intermediates have a similar 30% stimulation in WUE_i, while C_4-like and C_4 species show a more than tripling of their WUE_i stimulation at modern CO_2 levels (Fig. 5B).

If the marginal WUE is assumed to increase with atmospheric CO_2 (e.g. Katul *et al.*, 2010; Manzoni *et al.*, 2011), the predicted g_s at c_a=280 μmol mol^{-1} increases. As a consequence, photosynthesis also increases and the ratios of net photosynthesis at c_a=400 μmol m^{-2} s^{-1} and 280 μmol mol^{-1} therefore decrease (Fig. 4B). Because the positive effect of changes in λ is larger on transpiration than on net photosynthesis, the WUE_i at the lower c_a decreases. As a result, the ratio of WUE_i at current and low CO_2 concentrations is higher than when assuming a constant λ (Fig. 5B).

The modelled changes in leaf-level performance between photosynthetic groups under low c_a are shown in Fig. 6. This figure quantifies the advantages of the intermediate and C_4 species over the basal C_3 state. At low c_a, the estimated changes in η and λ for intermediate species provide a continuous, smooth gradient of increasing carbon gain, over a C_3 *Flaveria* species (Fig. 6A). This trend is robust to changes in the λ(c_a) relationship, as indicated by minor differences between filled and open symbols. A Type I intermediate has a 15% higher A_{net} than a C_3 species, which could provide a competitive edge to the intermediate in a low CO_2 environment; a similar jump in A_{net} is seen for each photosynthetic group along the evolutionary trajectory, in agreement with a recently proposed smoothly increasing fitness landscape for C_4 evolution (Heckmann *et al.*, 2013). However, the same pattern is not apparent in the WUE_i results (Fig. 6B). There is no difference in the WUE_i estimated at 280 μmol mol^{-1} CO_2 between C_3, Type I and Type II *Flaveria* species. Instead, significant increases in WUE_i are only achieved in C_4-like and C_4 species, implying that the driving force for the initial steps

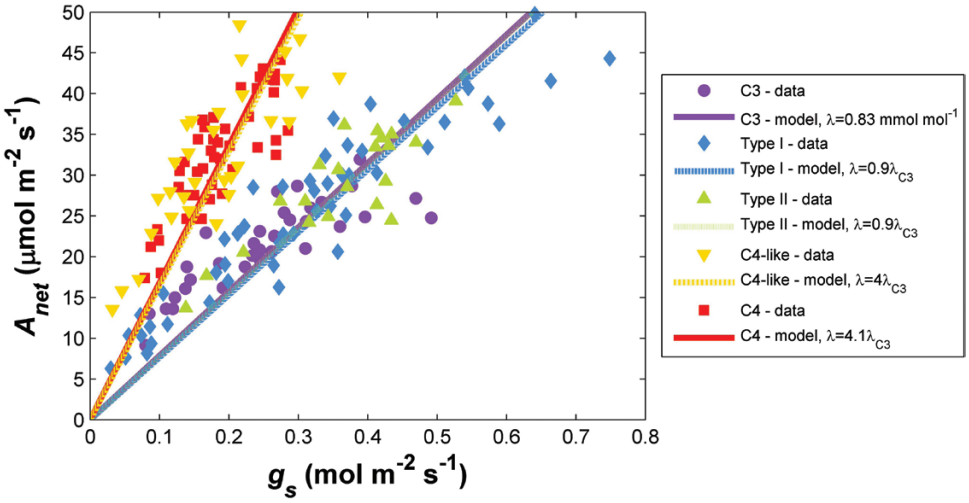

Fig. 3. Relationships between stomatal conductance to CO_2 (g_s) and net CO_2 assimilation rate (A_{net}) in *Flaveria* species across the C_3 to C_4 photosynthetic range. Data points are from Vogan and Sage (2011); lines are obtained by analytical least-square fitting of the water use efficiency λ, employing a linearized version of the stomatal optimization model (Manzoni *et al.*, 2011) for analytical tractability.

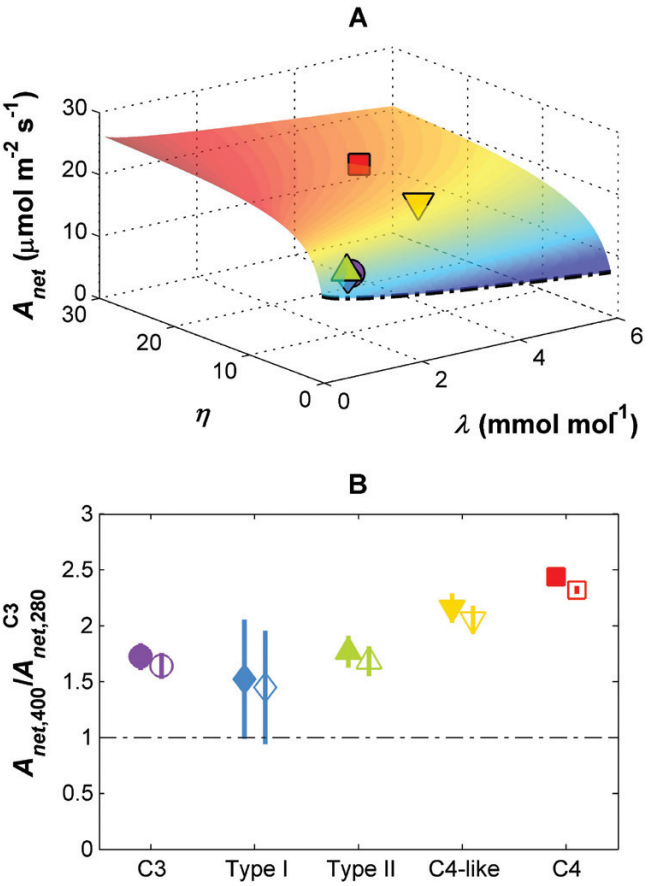

Fig. 4. (A) Modelled relationships between net CO_2 assimilation rate (A_{net}), marginal water use efficiency (λ), and the CO_2-concentrating pump strength (η) modelled at current CO_2 concentrations (400 μmol mol^{-1}); $V_{c,max}$, K_{cair}, and Γ* vary with η according to the relationships in Fig. 2; vapour pressure deficit (D) was set to 1.5 kPa, leaf temperature to 30 °C, Q to 1500 μmol m^{-2} s^{-1}. Mean values of λ and η for each of the five photosynthetic types are indicated on the surface. (B) The ratio of A_{net} at current atmospheric CO_2 levels versus A_{net} of C_3 *Flaveria* at low atmospheric CO_2 concentrations (280 μmol mol^{-1}) ($A_{net,400}/A^{C3}_{net,280}$) for each photosynthetic group; means ±SE across species; filled symbols refer to constant λ, open symbols to λ increasing linearly with c_a; the dashed-dotted line indicates a ratio of 1. C_3 species, purple circle; Type I species, blue diamond; Type II species, green triangle; C_4-like species, yellow inverted triangle; C_4 species, red square.

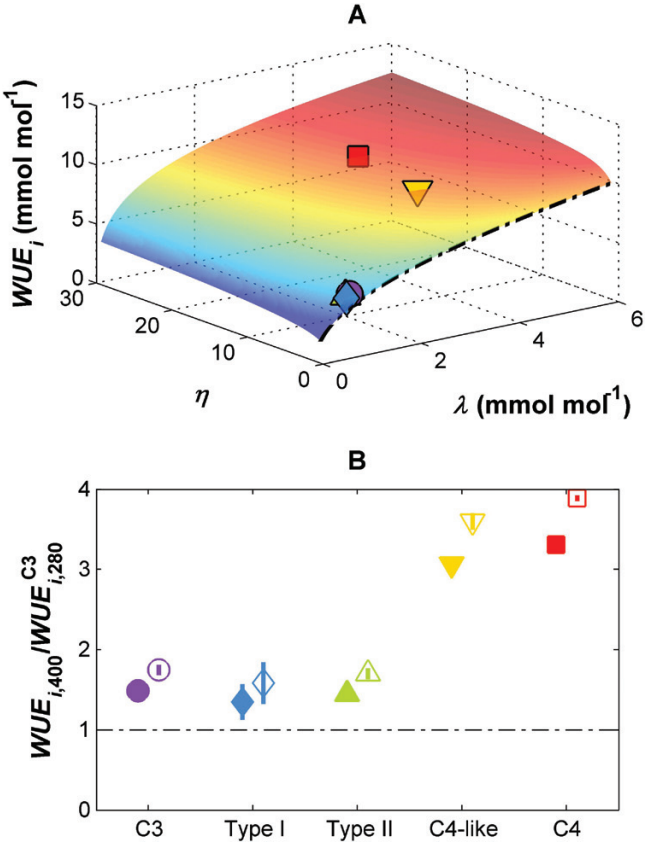

Fig. 5. Modelled relationships between instantaneous water use efficiency (WUE_i, the ratio of A_{net} to E), marginal WUE (λ), and the CO_2-concentrating pump strength (η) modelled at current CO_2 concentrations (400 μmol mol^{-1}); $V_{c,max}$, K_{cair}, and Γ* vary with η according to the relationships in Fig. 2; vapour pressure deficit (D) was set to 1.5 kPa, leaf temperature to 30 °C, Q to 1500 μmol m^{-2} s^{-1}. Mean values of λ and η for each of the five photosynthetic types are indicated on the surface. (B) The ratio of WUE_i at current atmospheric CO_2 levels versus the WUE_i of a C_3 *Flaveria* at low atmospheric CO_2 concentrations (280 μmol mol^{-1}) ($WUE_{i400}/WUE^{C3}_{i280}$) for each photosynthetic group; means ±SE across species; filled symbols refer to constant λ, open symbols to λ increasing linearly with c_a; the dashed-dotted line indicates a ratio of 1. C_3 species, purple circle; Type I species, blue diamond; Type II species, green triangle; C_4-like species, yellow inverted triangle; C_4 species, red square.

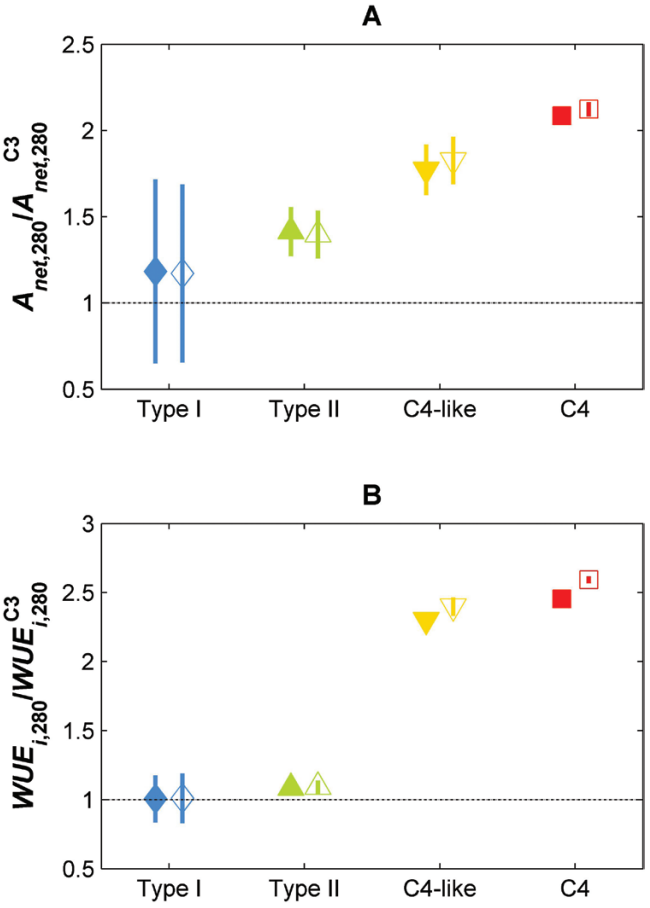

Fig. 6. Comparison of (A) modelled photosynthetic rates and (B) modelled WUE_i among *Flaveria* species with different photosynthetic types at c_a=280 μmol mol^{-1}, expressed as ratios over the mean A_{net} and WUE_i for C_3 species at c_a=280 μmol mol^{-1}. Symbols represent means ±SE across species (for fixed C_3 A_{net} and WUE_i values); filled symbols refer to constant λ, open symbols to λ increasing linearly with c_a; the dashed-dotted line indicates a ratio of 1. Other parameters are as in Figs 4 and 5.

towards C_4 photosynthesis in this group was carbon based and not related to increasing WUE_i.

Many of the features considered to pre-adapt a group to evolve C_4 photosynthesis are related to leaf hydraulics, including increased vein density and enlarged bundle sheath cell size (McKown *et al.*, 2005; McKown and Dengler, 2007; Osborne and Sack, 2012; Sage *et al.*, 2012; Griffiths *et al.*, 2013). Stomatal anatomy also evolves along the transition from C_3 to C_4 photosynthesis, with C_4 species having lower maximum stomatal conductance (due to either lower stomatal density or smaller stomatal size) than C_3 congeners (Taylor *et al.*, 2012). While changes in whole-plant physiology are outside the scope of this work, these findings have stimulated interest in the role of plant water relations in the evolution of C_4 photosynthesis. The results here indicate that while there is a gradual increase in carbon gain across the range from C_3 to C_4, there is no corresponding transition in either WUE_i or λ. Rather, increases in leaf-level WUE_i are only seen between Type II intermediacy and C_4-like species (as noted by Kocacinar *et al.*, 2008; Vogan and Sage, 2011). However, this transition is accompanied by a rise in λ, indicating that a higher carbon cost is being incurred for water loss in C_4-like and C_4 species than in C_3, or Type I or Type II intermediate species of *Flaveria*. This corresponds to the coordinated set of changes to the hydraulic architecture of *Flaveria* species, including lower leaf specific hydraulic conductivity and greater cavitation resistance in C_4 and C_4-like than C_3 species (Kocacinar *et al.*, 2008), emphasizing the importance of the transition from having a functional C_4 cycle for both the carbon and water economies of the plant.

Conclusions

Using a stomatal optimization approach, the full range of C_3, C_3–C_4 intermediates. and C_4 gas exchange could be realistically modelled with the addition of a C_4 pump strength parameter η, describing the effects of the C_4 carbon-concentrating mechanism. The results here showed that, to capture the patterns apparent in measured gas exchange data, the carbon-based cost of losing water (λ) between C_3, and Type I and Type II intermediates could be maintained constant, but λ had to be quadrupled to model C_4-like and C_4 *Flaveria* (at least within the confines of the optimality assumption of stomata). When leaf-level fluxes were modelled at low CO_2, there was no evidence for a greater WUE_i in the C_3–C_4 intermediates (compared with a C_3 *Flaveria*) until they developed a full C_4 cycle. However, the model results suggest a steady increase in net carbon fixation rates across the C_3 to C_4 photosynthetic range. While this implies that carbon, not water, was the main driving pressure for the early steps of C_4 evolution in this genus, the increase in λ indicates that there was a fundamental shift over the evolution of C_4 photosynthesis between the relative costs of carbon and water, resulting in higher carbon costs of water losses.

Supplementary data

Supplementary data are available at *JXB* online.
Table S1. Parameter table.

Acknowledgements

The authors would like to thank the editor, Rowan Sage, and two anonymous reviewers for their constructive comments on the paper. This work was supported by grants from the US Department of Agriculture, Agriculture and Food Research Initiative (#2011-67003-30222) and the US Department of Energy, Terrestrial Ecosystem Sciences (#11-DE-SC-0006967) to DAW and GGK, and from the US–Israeli Bi-national Science Foundation (#2010320) and the Natural Sciences and Engineering Research Council of Canada to DAW. GV gratefully acknowledges the support of the project 'AgResource – Resource Allocation in Agriculture', from the Faculty of Natural Resources and Agricultural Sciences, Swedish University of Agricultural Sciences (SLU); SM was supported through an excellence grant from the Faculty of Natural Resources and Agricultural Sciences and the vice-chancellor of the SLU.

References

Busch FA, Sage TL, Cousins AB, Sage RF. 2013. C3 plants enhance rates of photosynthesis by reassimilating photorespired and respired CO_2. *Plant, Cell and Environment* **36,** 200–212.

Campbell GS, Norman JM. 1998. *An introduction to environmental biophysics* , 2nd edn. Berlin: Springer.

Campbell CD, Sage RF, Kocacinar F, Way DA. 2005. Estimation of the whole-plant CO_2 compensation point of tobacco (*Nicotiana tabacum* L.). *Global Change Biology* **11,** 1956–1967.

Cheng L, Fuchigami LH, Breen PJ. 2001. The relationship between photosystem II efficiency and quantum yield for CO_2 assimilation is not affected by nitrogen content in apple leaves. *Journal of Experimental Botany* **52,** 1865–1872.

Christin PA, Osborne CP, Sage RF, Arakaki M, Edwards EJ. 2011. C_4 eudicots are not younger than C_4 monocots. *Journal of Experimental Botany* **62,** 3171–3181.

Collatz, GJ, Ribas-Carbo M, Berry JA. 1992. Coupled photosynthesis–stomatal conductance model for leaves of C4 plants. *Australian Journal of Plant Physiology* **19,** 519–538.

Cowan IR, Farquhar GD. 1977. Stomatal function in relation to leaf metabolism and environment. *Symposia of the Society for Experimental Biology* **31,** 471–505.

Dai Z, Ku MSB, Edwards GE. 1996. Oxygen sensitivity of photosynthesis and photorespiration in different photosynthetic types in the genus *Flaveria*. *Planta* **198,** 563–571.

Edwards GE, Ku MSB. 1987. Biochemistry of C3–C4 intermediates. In: Strumpf PK, Conn EE, eds.*The biochemistry of plants*. London: Academic Press, 275–325.

Ehleringer JR, Cerling TE, Helliker BR. 1997. C4 photosynthesis, atmospheric CO_2, and climate. *Oecologia* **112,** 285–299.

Farquhar G, von Caemmerer S, Berry JA. 1980. A biochemical model of photosynthetic CO_2 assimilation in leaves of C3 species. *Planta* **149,** 78–90.

Genty B, Briantais JM, Baker NR. 1989. The relationship between the quantum yield of photosynthetic electron transport and quenching of chlorophyll fluorescence. *Biochimica et Biophysica Acta* **990,** 87–92.

Gowik U, Bräutigam A, Weber KL, Weber APM, Westhoff P. 2011. Evolution of C4 photosynthesis in the genus *Flaveria*—how many and which genes does it take to make C4? *The Plant Cell* **23,** 2087–2105.

Gowik U, Westhoff P. 2011. The path from C_3 to C_4 photosynthesis. *Plant Physiology* **155,** 56–63.

Griffiths H, Weller G, Toy LF, Dennis RJ. 2013. You're so vein: bundle sheath physiology, phylogeny and evolution in C3 and C4 plants. *Plant, Cell and Environment* **36,** 246–261.

Hari P, Mäkelä A, Korpilahti E, Holmberg M. 1986. Optimal control of gas exchange. *Tree Physiology* **2,** 169–175.

Heckmann D, Schulze S, Denton A, Gowik U, Westhoff P, Weber APM, Lercher MJ. 2013. Predicting C4 photosynthesis evolution: modular, individually adaptive steps on a Mount Fuji fitness landscape. *Cell* **153,** 1579–1588.

Huxman TE, Monson RK. 2003. Stomatal responses of C3, C3–C4 and C4 *Flaveria* species to light and intercellular CO_2 concentration: implications for the evolution of stomatal behavior. *Plant, Cell and Environment* **26,** 313–322.

Kapralov MV, Kubien DS, Andersson I, Filatov DA. 2011. Changes in Rubisco kinetics during the evolution of C4 photosynthesis in *Flaveria* (Asteraceae) are associated with positive selection on genes encoding the enzyme. *Molecular Biology and Evolution* **28,** 1491–1503.

Katul G, Manzoni S, Palmroth S, Oren R. 2010. A stomatal optimization theory to describe the effects of atmospheric CO_2 on leaf photosynthesis and transpiration. *Annals of Botany* **105,** 431–442.

Kocacinar F, McKown AD, Sage TL, Sage RF. 2008. Photosynthetic pathway influences xylem structure and function in *Flaveria* (Asteraceae). *Plant, Cell and Environment* **31,** 1363–1376.

Krall JP, Edwards GE, Ku MSB. 1991. Quantum yield of photosystem II and efficiency of CO_2 fixation in *Flaveria* (Asteraceae) species under varying light and CO_2. *Australian Journal of Plant Physiology* **18,** 369–383.

Ku MSB, Wu J, Dai Z, Scott RA, Chu C, Edwards GE. 1991. Photosynthetic and photorespiratory characteristics of *Flaveria* species. *Plant Physiology* **96,** 518–528.

Kubien DS, Whitney SM, Moore PV, Jesson LK. 2008. The biochemistry of Rubisco in *Flaveria*. *Journal of Experimental Botany* **59,** 1767–1777.

Laisk A, Edwards GE. 2000. A mathematical model of C4 photosynthesis: the mechanism of concentrating CO_2 in NADP-malic enzyme type species. *Photosynthesis Research* **66,** 199–224.

Lloyd J, Farquhar GD. 1994. C-13 discrimination during CO_2 assimilation by the terrestrial biosphere. *Oecologia* **99,** 201–215.

Lüthi D, Le Floch M, Bereiter B, *et al*. 2008. High-resolution carbon dioxide concentration record 650,000–800,000 years before present. *Nature* **453,** 379–382.

Manzoni S, Vico G, Katul G, Fay PA, Polley W, Palmroth S, Porporato A. 2011. Optimizing stomatal conductance for maximum carbon gain under water stress: a meta-analysis across plant functional types and climates. *Functional Ecology* **25,** 456–467.

Manzoni S, Vico G, Palmroth S, Porporato A, Katul G. 2013. Optimization of stomatal conductance for maximum carbon gain under dynamic soil moisture. *Advances in Water Resources* **62,** 90–105.

McKown AD, Dengler NG. 2007. Key innovations in the evolution of Kranz anatomy and C_4 vein pattern in *Flaveria* (Asteraceae). *American Journal of Botany* **94,** 382–399.

McKown AD, Moncalvo JM, Dengler NG. 2005. Phylogeny of *Flaveria* (Asteraceae) and inference of C4 photosynthesis evolution. *American Journal of Botany* **92,** 1911–1928.

Monson RK. 1989. The relative contribution of reduced photorespiration, and improved water- and nitrogen-use efficiencies, to the advantages of C_3–C_4 intermediate photosynthesis in *Flaveria*. *Oecologia* **80,** 215–221.

Monson RK, Jaeger CH. 1991. Photosynthetic characteristics of the C3–C4 intermediate *Flaveria floridana* J.R. Johnson measured in its natural habitat. Evidence of the advantages to C3–C4 photosynthesis at high leaf temperatures. *American Journal of Botany* **78,** 795–800.

Morison JIL, Gifford RM. 1983. Stomatal sensitivity to carbon dioxide and humidity: a comparison of two C3 and two C4 grasses. *Plant Physiology* **71,** 789–796.

Osborne CP, Sack L. 2012. Evolution of C4 plants: a new hypothesis for an interaction of CO_2 and water relations mediated by plant hydraulics. *Philosophical Transactions of the Royal Society B: Biological Sciences* **367,** 583–600.

Rawson HM, Begg JE, Woodward RG. 1977. The effect of atmospheric humidity on photosynthesis, transpiration and water use efficiency of leaves of several plant species. *Planta* **134,** 5–10.

Ripley BS, Cunniff J, Osborne CP. 2013. Photosynthetic acclimation and resource use by the C3 and C4 subspecies of *Alloteropsis semialata* in low CO_2 atmospheres. *Global Change Biology* **19,** 900–910.

Sage RF. 2004. The evolution of C_4 photosynthesis. *New Phytologist* **161,** 341–370.

Sage RF, Sage TL, Kocacinar F. 2012. Photorespiration and the evolution of C4 photosynthesis. *Annual Review of Plant Biology* **63,** 19–47.

Sudderth EA, Muhaidat RM, McKown AD, Kocacinar F, Sage RF. 2007. Leaf anatomy, gas exchange and photosynthetic enzyme activity in *Flaveria kochiana*. *Functional Plant Biology* **34,** 118–129.

Taiz L, Zeiger E. 2010. *Plant physiology* , 5th edn. Sunderland, MA: Sinauer Associates.

Taylor SH, Ripley BS, Woodward FI, Osborne CP. 2011. Drought limitation of photosynthesis differs between C3 and C4 grass species in a comparative experiment. *Plant, Cell and Environment* **34,** 65–75.

Taylor SH, Franks P, Hulme S, Spiggs E, Christin P-A, Edwards E, Woodward I, Osborne C. 2012. Photosynthetic pathway and ecological adaptation explain stomatal trait diversity amongst grasses. *New Phytologist* **193,** 387–396.

Vico G, Manzoni S, Palmroth S, Weih M, Katul G. 2013. A perspective on optimal leaf stomatal conductance under CO_2 and light co-limitations. *Agricultural and Forest Meteorology* **182–183,** 191–199.

Vico G, Porporato A. 2008. Modelling C3 and C4 photosynthesis under water-stressed conditions. *Plant and Soil* **313,** 187–203.

Vogan PJ, Frohlich MW, Sage RF. 2007. The functional significance of C3–C4 intermediate traits in *Heliotropium* L. (Boraginaceae): gas exchange perspectives. *Plant, Cell and Environment* **30,** 1337–1345.

Vogan PJ, Sage RF. 2011. Water-use efficiency and nitrogen-use efficiency of C3–C4 intermediate species of *Flaveria* Juss. (Asteraceae). *Plant, Cell and Environment* **34,** 1415–1430.

von Caemmerer S. 1989. A model of photosynthetic CO_2 assimilation and carbon-isotope discrimination in leaves of certain C3–C4 intermediates. *Planta* **178,** 463–474.

von Caemmerer S. 2000. *Biochemical models of leaf photosynthesis*. Collingwood, Victoria: CSIRO.

von Caemmerer S. 2013. Steady state models of photosynthesis. *Plant, Cell and Environment* **36,** 1617–1630.

Way DA. 2012. What lies between: the evolution of stomatal traits on the road to C_4 photosynthesis. *New Phytologist* **193,** 291–293.